

# Size-dependent particulate matter indoor/outdoor relationships for a wind-induced naturally ventilated airspace

Chung-Min Liao<sup>a,\*</sup>, Su-Jui Huang<sup>a</sup>, Hsin Yu<sup>b</sup>

<sup>a</sup>Department of Bioenvironmental Systems Engineering, National Taiwan University, Taipei, Taiwan 10617, ROC

<sup>b</sup>Department of Civil Engineering, National Ilan University, Ilan, Taiwan 260, ROC

Received 26 November 2002; received in revised form 26 August 2003; accepted 26 September 2003

## Abstract

We applied a simple size-dependent indoor air quality model associated with measured outdoors particulate matter (PM) profiles and potential loss mechanisms to characterize PM indoor/outdoor (I/O) relationships for wind-induced naturally ventilated residences in Taiwan region. The natural ventilation rate was quantified by the opening effectiveness for sidewall opening and covered ridge with sidewall-opening-type homes. The measured results demonstrate that integrated PM<sub>10</sub> and PM<sub>2.5</sub> mass concentrations for the urban area are 39.2 and 3.13  $\mu\text{g m}^{-3}$ , respectively, whereas for the suburban area are 75.76 and 69.87  $\mu\text{g m}^{-3}$ , respectively. The most significant removal mechanisms included natural ventilation through and particle deposition on indoor surfaces. The predicted average PM mass I/O ratios were 0.56 and 0.42 for PM<sub>2.5</sub> and PM<sub>10</sub>, respectively. We also employed published data on mass-weighted size distributions for specific chemical constituents of PM, sulfate and nitrate, to predict PM I/O ratios in the central Taiwan region; the resulting values ranged from 0.22 to 0.43 and 0.27 to 0.36 for sulfate and nitrate, respectively. Our results demonstrate that the PM I/O ratios for a wind-induced natural ventilated airspace depend strongly on the ambient particle distributions, building openings design (e.g. height-to-length ratio of openings and roof slope), wind speed, wind angle of incidence, and outdoor PM metrics.

© 2003 Elsevier Ltd. All rights reserved.

**Keywords:** Particulate matter; Deposition; Natural ventilation; Opening effectiveness; Indoor/outdoor ratio; Modeling

## 1. Introduction

Outdoor particulate matter (PM) present on the surface of streets may consist of a complex mixture of soil dust, deposited motor vehicle exhaust particles, tire dust, brake lining wear dust, plant fragments, and other biological materials. Pope and Dockery [1], Dockery et al. [2], Schwartz [3], Seaton et al. [4], and Ackermann-Liebrich et al. [5] in their epidemiological studies indicated that the PM in outdoor air was strongly associated with lung function parameters, respiratory symptoms and mortality. These findings were especially pronounced for inhaled thoracic particles (particles of aerodynamic equivalent diameter (AED) less than 10  $\mu\text{m}$ , PM<sub>10</sub>) and fine particles (particles smaller than 2.5  $\mu\text{m}$  AED, PM<sub>2.5</sub>).

Guo et al. [6] revealed that PM<sub>10</sub> was positively associated with the prevalence of asthma in middle-school students in Taiwan. Hwang and Chen [7] demonstrated that the rates of daily clinic visits were associated with current-day concentrations of PM<sub>10</sub> in Taiwan region. As most time of 70–90% is spent indoors, information on the indoor and outdoor relationships of PM concentrations is important. Indoor PM attributable to the outdoor air in urban/suburban residence houses has been the most serious indoor air pollution in Taiwan region [8–14]. In the indoor environment, the removal of entrained outdoor PM occurs through ventilation and deposition. The types of ventilation, the outdoor levels, and climate can influence indoor PM concentrations.

Natural ventilation is widely used in Taiwan region with the advantages of saving energy, expense, and installation time in that dwelling houses are controlled by natural convection to remove excessive heat and moisture. The mechanism of natural ventilation depends on wind effects, thermal buoyancy and the combination of both wind and buoyancy

\* Corresponding author. Tel: +886-2-2363-4512; fax: +886-2-2362-6433.

E-mail address: [cmliao@ccms.ntu.edu.tw](mailto:cmliao@ccms.ntu.edu.tw) (C.-M. Liao).

forces. Wind speed and wind direction are the dominant factors for wind-induced effects. de Jong and Bot [15] and Miguel et al. [16] indicated that a full understanding of the relationship between wind characteristics (wind speed and wind direction) and ventilation characteristics (dimensions, inlet and outlet design, etc.) are required to achieve sufficient natural ventilation. The most popular types of natural ventilation openings employed in Taiwan region are windows, doors, and roof ventilators. The characteristics of openings affect natural ventilation efficiency with the arrangement, location, and control of ventilation openings to achieve a desired ventilation rate and good distribution of ventilation air through the buildings [17,18]. Therefore, a study of the indoor PM removal from a wind-induced naturally ventilated airspace is of fundamental and practical significance.

In a naturally ventilated airspace, Brownian and turbulent diffusion, sedimentation, and laminar as well as convective flow exist to varying degrees and lead to particle deposition onto walls and other surfaces. Depending on the flow regime, different models have been proposed for particle deposition in a ventilated airspace. The turbulent flow scheme appears to be best applicable to a naturally ventilated airspace in which turbulent flow is a typical feature of the airflow. In the present work, we adopted a mathematical model derived by Crump and Seinfeld [19] for the rate of aerosol deposition in a turbulence-mixing enclosure of arbitrary shape under the assumption of homogeneous turbulent near the surfaces.

Indoor sources such as environmental tobacco smoke, cooking, and cleaning activities can contribute significantly to indoor PM levels in that these indoor sources require a further research to characterize their effects [20,21]. Since the epidemiological literature has focused on health effects associated with ambient particle levels, we do not include indoor source in our analysis and focus on the PM indoor/outdoor (I/O) relationships. Thatcher and Layton [22] indicated that resuspension would also affect the PM I/O relationships; this effect would be most pronounced for coarse mode particles (such as PM<sub>2.5–10</sub>). We do not include the effects of resuspension in the present work since more research is required to thoroughly characterize this effect.

In this study, we attempt to understand the PM I/O relationships focusing on the building operational characteristics of a wind-induced naturally ventilated airspace and the size-dependent effects on indoor PM levels. We performed an opening effectiveness concept to quantify the wind-induced natural ventilation for sidewall openings and covered ridge with sidewall openings that are commonly employed in Taiwan region. We predicted the size-dependent I/O ratios of PM mass and selected chemical species of sulfate and nitrate for urban and suburban naturally ventilated homes, and compared our results with empirical evidence. Our results of the predicted PM I/O ratios can also be incorporated with health-risk-assessment framework, i.e., hazard identification, exposure profile, dose–response profile, and risk characteristics to evaluate the human exposure and risk assessment in an indoor environment.

## 2. Materials and methods

### 2.1. Model for PM I/O relationships

Thatcher and Layton [22], Abt et al. [20], and Riley et al. [23] have developed rigorous indoor air-quality models for studying the PM I/O relationships and size-dependent removal mechanisms in a residence, in which the model employed by them applied also to our study. Combining the physical processes controlling the gain and loss rates, the deposition (including Brownian and turbulent diffusive deposition and gravitational sedimentation), and air exchange, yields a dynamic equation that describes the concentration profile of PM I/O relationships in a wind-induced naturally ventilated airspace.

Followed by the principle of mass balance under an isothermal condition in that resuspension, coagulation of particles, and phase change processes are neglected, the dynamic equation varying with particle size range  $k$  and time  $t$  is given by

$$\frac{dC(k,t)}{dt} = -(\lambda_n + \lambda_d(k))C(k,t) + \lambda_n C_o(k,t),$$

$$k = 1, 2, A, N - 1, \quad (1)$$

where  $C(k,t)$  is the time-dependent indoor PM concentration in the  $k$ th size range ( $\text{kg m}^{-3}$ );  $C_o(k,t)$  is the time-dependent outdoor PM concentration in the  $k$ th size range ( $\text{kg m}^{-3}$ );  $\lambda_n$  is the air exchange rate of natural ventilation through open windows and doors ( $\text{h}^{-1}$ ) in which  $\lambda_n = Q_n/V$ ,  $Q_n$  is the natural ventilation rate ( $\text{m}^3 \text{h}^{-1}$ );  $V$  is the air volume ( $\text{m}^3$ );  $\lambda_d(k)$  is the deposition rate of indoor PM due to Brownian and turbulent diffusive deposition and gravitational sedimentation in the  $k$ th size range ( $\text{h}^{-1}$ );  $k$  is the size range number; and  $N$  is assigned to be the end point number for a  $k$ th size range,  $d_k$  and  $d_{k+1}$ .

The particles are divided into geometrically equal sized bins in the size range of interest. The PM concentration is assumed to be a constant AED within each bin size. The end points,  $d_k$  and  $d_{k+1}$ , of the  $k$ th bin size are considered to be equal to the geometric mean of the end points of the bin size as,

$$d_k = d_{\min} + \frac{(d_{\max} - d_{\min})(k - 1)}{N - 1}, \quad k = 1, 2, A, N, \quad (2)$$

where particles smaller than  $d_{\min}$  (the minimum diameter) are considered to be the finest, and  $d_{\max}$  is the largest particle size of interest.

Applying a time average to Eq. (1), whereas neglecting the change of PM mass within the building and assuming that  $C_o$  and  $C$  are not correlated in time with  $Q_n$  or  $\lambda_d(k)$ , yields

$$\frac{C(k)}{C_o(k)} = \frac{\lambda_n}{\lambda_n + \lambda_d(k)}, \quad (3)$$

where  $C(k)/C_o(k)$  is the size-specific, time-averaged PM I/O concentration ratio. Eq. (3) also describes the

Table 1  
Rate equations of PM deposition model in a naturally ventilated airspace

$$\lambda_d(k) = \frac{1}{d_{k+1} - d_k} \int_{d_k}^{d_{k+1}} \lambda_d(d_p) d(d_p) \quad (\text{T.1})$$

where

$$\lambda_d(d_p) = \frac{1}{lwh} \left\{ (2wh + 2hl) \left( \left( \sin \frac{\pi}{n} \right) (k_e D(d_p)^{n-1})^{1/n} \right) + wlv_s(d_p) \coth \left( \frac{\pi v_s(d_p)}{2(n \sin \frac{\pi}{n}) (k_e D(d_p)^{n-1})^{1/n}} \right) \right\} \quad (\text{T.2}^a)$$

$$D(d_p) = \frac{k_B T C_{\text{slip}}}{3\pi\eta_a d_p} \quad (\text{T.3}^b)$$

$$v_s(d_p) = \frac{\rho_p g d_p^2}{18\eta_a} C_{\text{slip}} \left[ 1 - \frac{\rho_a}{\rho_p} \right] \quad (\text{T.4}^b)$$

$$\text{Slip correlation factor: } C_{\text{slip}} = \left( 1 + \frac{\lambda}{d_p} \left( 2.541 + 0.8 \exp \left( -0.55 \frac{d_p}{\lambda} \right) \right) \right) \quad (\text{T.5}^b)$$

<sup>a</sup>Derived from Crump and Seinfeld [19].

<sup>b</sup>Adopted from Hinds [34].

size-specific PM I/O concentration ratio for a particular chemical constitute of PM.

## 2.2. PM deposition model

The deposition model used to describe indoor PMs deposit in a naturally ventilation airspace is derived from Crump and Seinfeld [19], and is referred to as the C-S model. Depending on the flow regime, different models have been proposed for particle deposition in a room. The turbulent flow paradigm appears to be best applicable to the building scenario where ventilation (natural or forced) is the primary source of turbulent. The C-S model is a well-established general model for the rate of aerosol deposition due to turbulent diffusion, Brownian diffusion, and gravitational sedimentation in a turbulently mixed arbitrary shape of airspace. Detailed derivation of the deposition model can be found in Liao et al. [24].

The C-S model was developed for reactor vessels where turbulence is produced by stirring. The turbulence parameter ( $k_e$ ) was estimated by assuming complete turbulent dissipation of the input energy. It is difficult to estimate  $k_e$  when turbulence is induced by natural ventilation. Lai and Nazaroff [25] developed a mathematical model (referred to as the L-N model) for predicting indoor particle deposition from turbulent flow onto smooth surfaces. The L-N model yielded predictions that are consistent with the C-S model in that the best fit occurred with  $n = 2.95$  and  $k_e = 0.784$ , the maximum deviation is 2.6% over the range  $0.0001 \mu\text{m} \leq d_p \leq 10 \mu\text{m}$ . The parameter values used in the deposition model include dynamic viscosity of air ( $\eta_a$ ) =  $1.85 \times 10^{-4}$  aP, air density ( $\rho_a$ ) =  $1.18 \times 10^{-3}$  g cm<sup>-3</sup>, indoor absolute temperature ( $T$ ) = 300° K, Boltzmann's constant ( $k_B$ ) =  $1.38 \times 10^{-16}$  dyn cm<sup>2</sup> C<sup>-1</sup>, mean free path of air ( $\lambda$ ) =  $6.6 \times 10^{-6}$  cm, and particle density ( $\rho_p$ ) = 1.0 g cm<sup>-3</sup>. The main features of the PM deposition model in the naturally ventilated airspace are listed in Table 1. The relationships between deposition rate and AED under different surface area-to-volume ratio is illustrated in Fig. 1.

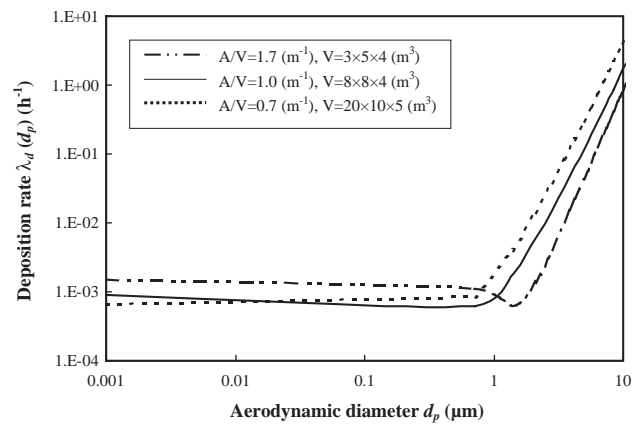


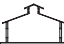

Fig. 1. The relationships of PM deposition rate and AED under different area surface-to-volume ratios.

## 2.3. Opening effectiveness model

The natural ventilation rate ( $Q_n$ ) depends on the effect of wind moving through openings. ASHRAE [17] suggests an empirical expression to predict the flow through a sidewall opening as a function of wind speed and opening effectiveness as:  $Q_n = EAV_w$ , where  $E$  is the opening effectiveness (dimensionless),  $A$  is the area of inlet opening (m<sup>2</sup>), and  $V_w$  is the wind velocity (m s<sup>-1</sup>). The traditional Buckingham Pi theorem is commonly used to derive an empirical relationship between the opening effectiveness and variables in terms of dimensionless parameters. The dimensionless parameters selected in the present study include: (i) the Reynolds number (Re) defined by the opening length, air density, air velocity, and absolute air viscosity; (ii) the ratio between opening height and opening length ( $h_0/l_0$ ); (iii) the incidence angle of wind flow ( $\phi$ ); and (iv) the slope of roof ( $\theta$ ). The detailed algorithm for developing the opening effectiveness model can be found in Yu et al. [26]. The expressions of opening effectiveness for the Sp- and CRSP-type buildings,  $E_{\text{SP}}$  and  $E_{\text{CRSP}}$ , respectively, can

Table 2

Parameters used to determine the opening effectiveness for two building types in urban and suburban in north (Taipei) and central Taiwan region

Building type	$V^a$	$h_0/l_0^a$	$\theta^a$	Wind speed <sup>b</sup> (wind direction)		Opening effectiveness ( $E$ )	
				North	Central	North	Central
CRSP type 	$8 \times 8 \times 4$	2/3	23.5°	$2.8 \pm 0.36$ (E) <sup>c</sup>	$1.7 \pm 0.22$ (N) <sup>c</sup>	0.50	0.65
SP type 	$8 \times 8 \times 4$	1/3	30°	$2.8 \pm 0.36$ (E) <sup>c</sup>	$1.7 \pm 0.22$ (N) <sup>c</sup>	0.47	0.60

<sup>a</sup> $V$  = volume (m<sup>3</sup>),  $h_0/l_0$  = Height-to-length ratio,  $\theta$  = roof slope angle.<sup>b</sup>Monthly averaged wind speed (mean  $\pm$ sd) in m s<sup>-1</sup>.<sup>c</sup>Monthly averaged wind direction, in which the mean incidence of wind angle ( $\phi$ ) is 90°.

be obtained as follows [26]:

$$E_{SP} = 7.44 \pm 1.2 \times (0.2Re)^{-0.35 \pm 0.08} \times (4h_0/l_0)^{0.10 \pm 0.06} \times (\sin \phi)^{0.75 \pm 0.19} \times (\sin \theta)^{-0.15 \pm 0.04}, \quad (4)$$

$$E_{CRSP} = 33.81 \pm 3.6 \times (0.4Re)^{-0.39 \pm 0.07} \times (3.2h_0/l_0)^{0.10 \pm 0.02} \times (\sin \phi)^{0.88 \pm 0.10} \times (\sin \theta)^{1.04 \pm 0.09}. \quad (5)$$

Table 2 gives the configuration parameters used in the present study for determining the opening effectiveness for the sidewall opening (SP) and the covered ridge sidewall opening (CRSP) type buildings located at north and central Taiwan region in that monthly averaged data of wind speed and wind direction were obtained from Taiwan EPA.

#### 2.4. Outdoor PM measurements

We selected urban and suburban areas located at north Taiwan (Taipei) region as study sites. The general urban site represents normal urban conditions without any specific air-pollution sources, whereas the suburban site represents the industrial area and the air quality mainly contributed by mobile sources. The ambient particle concentrations were measured in the periods of April 2001 in that the field 24-h samples were continuously collected over a weeklong period in the monitoring month. We also conducted a chamber test to verify the particle size distributions of the outdoor PM samples.

A portable laser dust monitor (Series 1100, Grimm Labor Technik GmbH & Co. KG, Ainring, Germany; referred to as DM1100) was used to analyze the PM characteristics. The DM1100 combines the principles of aerodynamic particle size separation and light-scattering particle detection. The DM1100 measured mass concentrations in the range of 1.0–50,000  $\mu\text{g m}^{-3}$ . Measured channels are in the ranges of < 0.5, 0.5–1, 1–2, 2–5, 5–10, and > 10  $\mu\text{m}$  AED. Before the measurements, the DM1100 was calibrated with known particles of Uniform Latex Microspheres Polystyrene (0.5  $\mu\text{m}$ ) and Polymer Microspheres Styrene

Table 3

Measured outdoor PM profile, particle concentrations in each bin and integrated PM metric mass concentrations collected from urban and suburban areas in north Taiwan (Taipei) region

	Urban	Suburban
<i>Measured outdoor PM profile</i>		
Particle size distribution	LN(1.06, 2.62) <sup>a</sup>	LN(0.56, 1.73) <sup>a</sup>
Particle concentration (m <sup>-3</sup> )	$1.36 \times 10^6$	$1.06 \times 10^7$
<i>Calculated particle concentration in each bin (m<sup>-3</sup>)</i>		
Bin 1 (0.1–1 $\mu\text{m}$ )	$5.7 \times 10^5$	$5.3 \times 10^6$
Bin 2 (1–2 $\mu\text{m}$ )	$3.9 \times 10^5$	$4.8 \times 10^6$
Bin 3 (2–3 $\mu\text{m}$ )	$1.4 \times 10^5$	$3.1 \times 10^5$
Bin 4 (3–4 $\mu\text{m}$ )	$7.9 \times 10^4$	$3.1 \times 10^4$
Bin 5 (4–5 $\mu\text{m}$ )	$5.4 \times 10^4$	$4.4 \times 10^3$
Bin 6 (5–6 $\mu\text{m}$ )	$4.8 \times 10^4$	$8.0 \times 10^2$
Bin 7 (6–7 $\mu\text{m}$ )	$3.6 \times 10^4$	$1.8 \times 10^2$
Bin 8 (7–8 $\mu\text{m}$ )	$2.4 \times 10^4$	45.2
Bin 9 (8–9 $\mu\text{m}$ )	$1.2 \times 10^4$	4.1
Bin 10 (9–10 $\mu\text{m}$ )	$6.1 \times 10^3$	2.0
<i>Calculated integrated mass concentration (<math>\mu\text{g m}^{-3}</math>)</i>		
PM <sub>2.5</sub>	3.13	69.87
PM <sub>2.5–10</sub>	36.1	6.18
PM <sub>10</sub>	39.2	75.76

<sup>a</sup>Lognormal distribution with a geometric mean diameter (GMD) and a geometric standard deviation (GSD): LN(GMD, GSD).

Vinyltoluene (3  $\mu\text{m}$ ) (Duke Scientific, Palo Alto, CA). The DM1100 was operated at the design sampling flow rate of  $1.2 \text{ l min}^{-1} \pm 10\%$ . The outputs from DM1100 can be expressed both as  $\mu\text{g m}^{-3}$  and as particles l<sup>-1</sup>. A portable IBM PC was used to collect all sampling data.

The results demonstrate that the particle size distributions of outdoor PM followed a lognormal distribution with a geometric mean diameter (GMD) of 1.06  $\mu\text{m}$  and a geometric standard deviation (GSD) of 2.62 for urban area, whereas a GMD of 0.56  $\mu\text{m}$  and 1.73 GSD for suburban area. The integrated PM<sub>10</sub> and PM<sub>2.5</sub> mass concentrations for the urban area are 39.2 and 3.13  $\mu\text{g m}^{-3}$ , respectively, whereas for the suburban area are 75.76 and

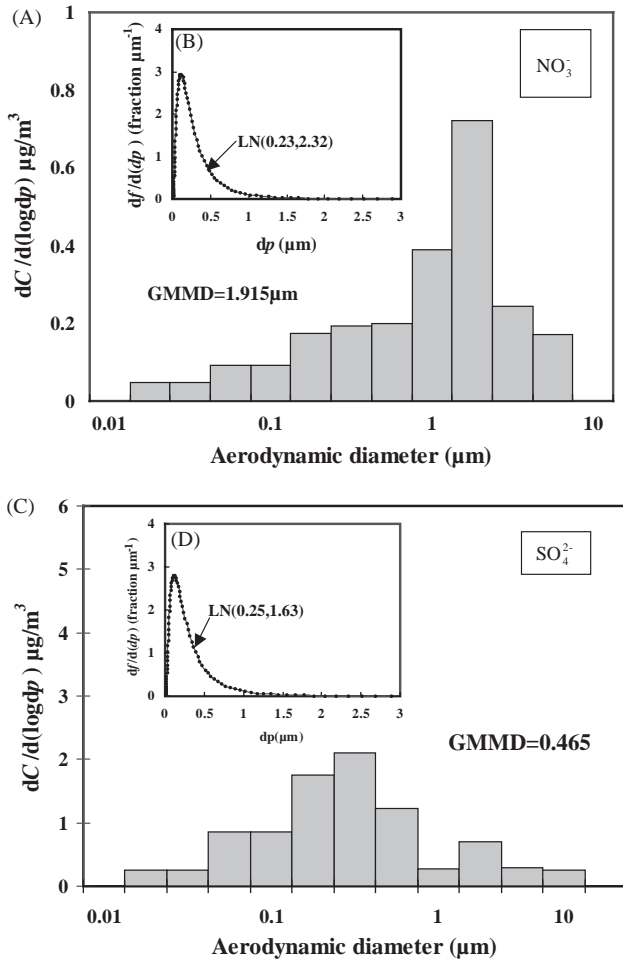


Fig. 2. Size-dependent sulfate ( $\text{SO}_4^{2-}$ ) and nitrate ( $\text{NO}_3^-$ ) concentrations collected from the central Taiwan region by Chang et al. [27] (A, C), in which the fitted lognormal models show the particle size distributions for sulfate and nitrate (B, D).

$69.87 \mu\text{g m}^{-3}$ , respectively. Table 3 summarizes the information of the lognormal modes for characteristic outdoor PM distributions in urban and suburban areas in Taipei region.

Since human health effects of ambient PM may depend on particle composition and size distribution, we developed PM I/O relationships for particles of different composition. Fang et al. [10] conducted an atmospheric aerosol sampling to characterize the chemical species in  $\text{PM}_{10}$  and  $\text{PM}_{2.5}$  aerosol from June to September in the suburban and rural sites of central Taiwan region. Results demonstrated that the dominant constituents in PM were sulfate and nitrate for the suburban and rural sites in central Taiwan. We present results here for two constituents: sulfate and nitrate. Chang et al. [27] conducted ambient air particle concentration samplings during July–October 2000 at a traffic site in central Taiwan to characterize the particle size distribution of sulfate and nitrate. We used the lognormal distribution to fit their size composition data, resulting in geometric mass mean diameters (GMMD) of 1.915 and 0.465  $\mu\text{m}$  for nitrate and

Table 4

Fitted outdoor PM profile, calculated particle concentrations in each bin and integrated PM metric mass concentrations of chemical species of sulfate and nitrate in central Taiwan region based on measurements of Fang et al. (1999) and Chang et al. (2001)

	Sulfate ( $\text{SO}_4^{2-}$ )	Nitrate ( $\text{NO}_3^-$ )
<i>Calculated outdoor PM sulfate and nitrate profile</i>		
Particle size distribution	LN(0.23, 2.32) <sup>a</sup>	LN(0.25, 1.63) <sup>a</sup>
Particle concentration ( $\text{m}^{-3}$ )	$2.3 \times 10^4$	$4.3 \times 10^3$
<i>Calculated particle concentration in each bin (<math>\text{m}^{-3}</math>)</i>		
Bin 1 (0.1–1 $\mu\text{m}$ )	$2.3 \times 10^4$	$4.3 \times 10^3$
Bin 2 (1–2 $\mu\text{m}$ )	$1.9 \times 10^{-1}$	$2.7 \times 10^{-1}$
Bin 3 (2–3 $\mu\text{m}$ )	$8 \times 10^{-2}$	$8 \times 10^{-2}$
Bin 4 (3–4 $\mu\text{m}$ )	$8 \times 10^{-2}$	$8 \times 10^{-2}$
Bin 5 (4–5 $\mu\text{m}$ )	$6.6 \times 10^{-3}$	$5 \times 10^{-3}$
Bin 6 (5–6 $\mu\text{m}$ )	$2 \times 10^{-4}$	$1.36 \times 10^{-3}$
Bin 7 (6–7 $\mu\text{m}$ )	$2 \times 10^{-4}$	$1.36 \times 10^{-3}$
Bin 8 (7–8 $\mu\text{m}$ )	$2 \times 10^{-4}$	$1.36 \times 10^{-3}$
Bin 9 (8–9 $\mu\text{m}$ )	$2 \times 10^{-4}$	$1.36 \times 10^{-3}$
Bin 10 (9–10 $\mu\text{m}$ )	$2 \times 10^{-4}$	$1.36 \times 10^{-3}$
<i>Calculated integrated mass concentration (<math>\mu\text{g m}^{-3}</math>)</i>		
$\text{PM}_{2.5}$	6.83	1.45
$\text{PM}_{2.5-10}$	0.89	0.77
$\text{PM}_{10}$	7.73	2.22

<sup>a</sup>Lognormal distribution with a geometric mean diameter (GMD) and a geometric standard deviation (GSD): LN(GMD, GSD).

sulfate, respectively (Figs. 2a, c). Figs. 2b, d show that the fitted lognormal particle size distributions are a 0.23  $\mu\text{m}$  GMD with a 2.32 GSD for nitrate, whereas a 0.25  $\mu\text{m}$  GMD with a 1.63 GSD for sulfate. Table 3 summarizes the information of lognormal modes for characteristic outdoor PM distributions of nitrate and sulfate in central Taiwan.

We computed integrated number ( $\text{cm}^{-3}$ ), surface area ( $\mu\text{m}^2 \text{cm}^{-3}$ ), volume ( $\mu\text{m}^3 \text{cm}^{-3}$ ), and mass ( $\mu\text{g m}^{-3}$ ) concentrations for three particles size ranges of  $\text{PM}_{2.5}$ ,  $\text{PM}_{2.5-10}$ , and  $\text{PM}_{10}$  by numerically integrating the appropriately weighted moment of the size distribution over the respective particle size range. We divided the size range from 0.1 to 10  $\mu\text{m}$  into 10 geometrically average size bins based on Eq. (2), in which the particle concentration in each bin was also calculated (Tables 3 and 4).

### 3. Results and discussion

Fig. 3 illustrates the outdoor and predicted indoor number, surface, and volume concentrations for the urban and suburban distributions in Taipei region for two building types. The overall influence of opening effectiveness and deposition differ among the number, surface area, and volume distributions because each PM metric has different size dependence. A large fraction of the urban and suburban number concentration distribution below particle AED of 3  $\mu\text{m}$  exists, indicating that the removal mechanisms are inefficient in the accumulation mode and unaffected by the building types (Figs. 3a, b). A large portion of the urban PM

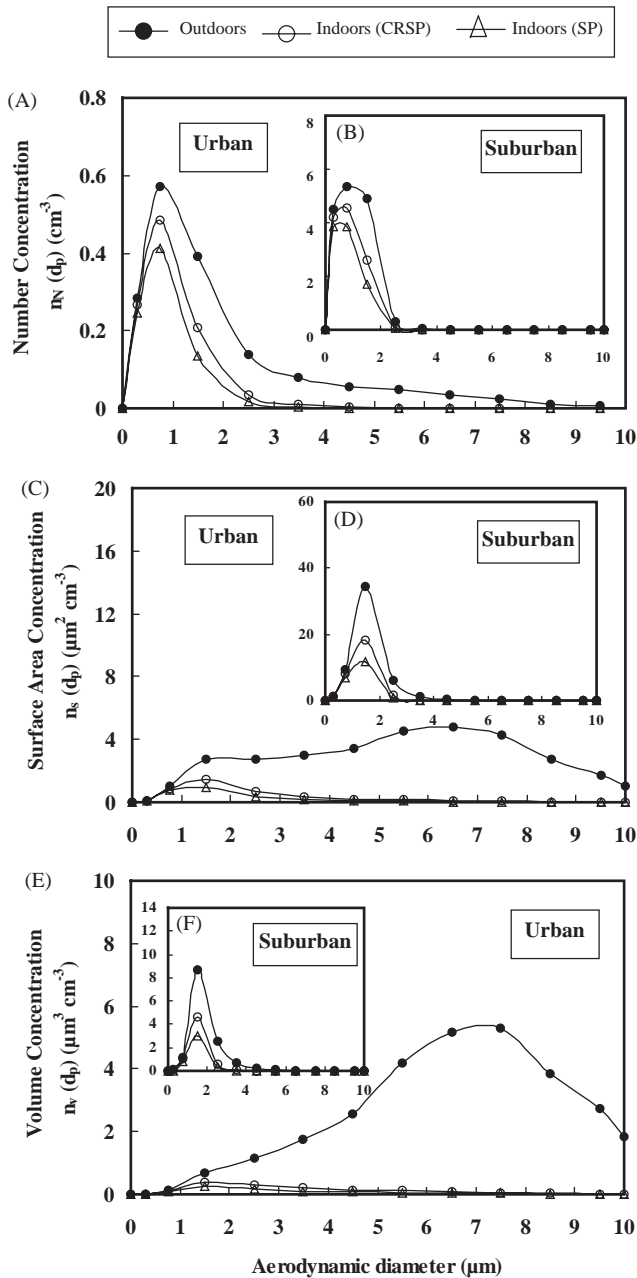


Fig. 3. Outdoor PM distributions of urban and suburban areas in north Taiwan (Taipei) region and predicted indoor PM number, surface area, and volume concentrations for the Sp- and CRSP-type buildings. (A, C, E) show the number, surface volume, and volume distributions, respectively, for urban PM; (B, D, F) show the corresponding distributions for suburban PM.

surface area and volume concentrations is removed (Figs. 3c, e), indicating both deposition and air exchange are efficient removal mechanisms; yet, this phenomenon does not occur in the suburban conditions (Figs. 3d, f). Fig. 3 also demonstrates that the SP-type building substantially reduces the indoor PM surface area and volume concentrations for both urban and suburban conditions more efficient than that of the CRSP-type building resulting from the SP-type build-

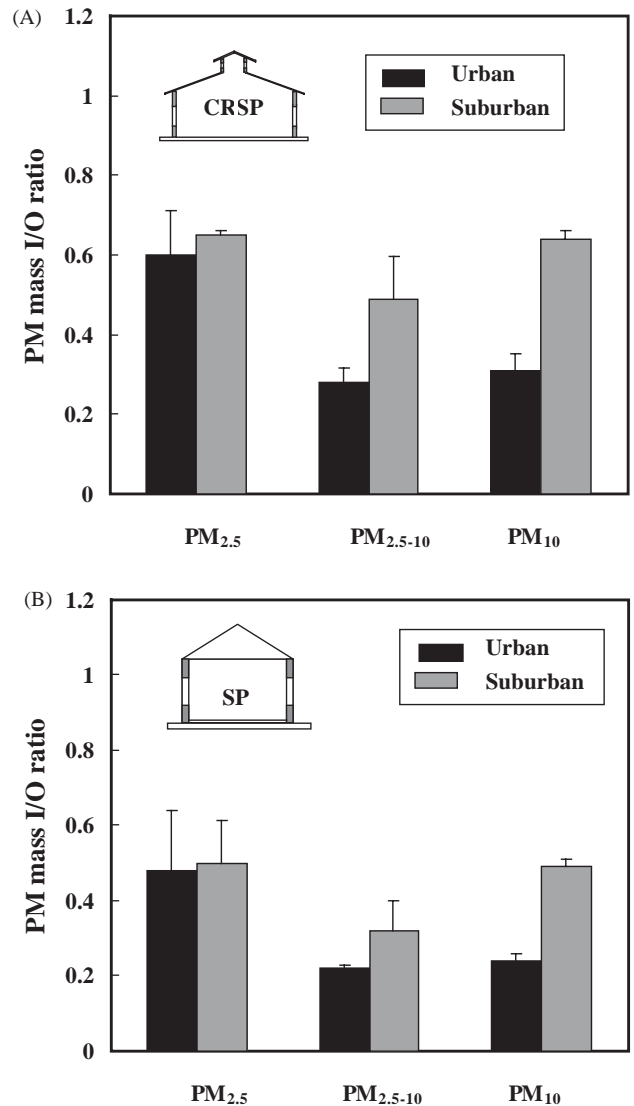


Fig. 4. Predicted PM mass I/O ratios of PM<sub>2.5</sub>, PM<sub>2.5-10</sub>, and PM<sub>10</sub> for (A) the Sp- and (B) the CRSP-type buildings in the urban and suburban areas of north Taiwan region. The error bars show the standard deviation from the mean.

ing has lower air exchange rate than that of CRSP-type. Much of the PM surface area and volume concentrations in the urban area is in the coarse mode (Figs. 3c, e), resulting in a large removal of PM<sub>10</sub> surface area and volume concentrations in both Sp- and CRSP-type buildings. For the suburban condition, both Sp- and CRSP-type buildings do not substantially reduce the PM surface area and volume concentrations (Figs. 3d, f).

Fig. 4 shows the PM mass I/O ratio predictions for Sp- and CRSP-type buildings in the urban and suburban areas of Taipei region. Values range from 0.22 for the PM<sub>2.5-10</sub> mass for SP-type building in urban area to 0.65 for CRSP-type building in suburban area (Table 5). Suburban area has higher PM mass I/O ratios than that in urban area. The SP-type building has lower PM mass I/O ratios than that of

Table 5

Predicted PM<sub>2.5</sub>, PM<sub>2.5–10</sub> and PM<sub>10</sub> mass indoor/outdoor (I/O) ratios (mean ±s.d.) for urban and suburban areas in north Taiwan region and for sulfate and nitrate in central Taiwan region for SP- and CRSP-type buildings

Location	Building type <sup>a</sup>	Air-exchange rate (mean ±s.d.) ( $\lambda_n, s^{-1}$ )	I/O ratio <sup>b</sup> = $\frac{\lambda_n}{\lambda_n + \lambda_d(k)}$		
			PM <sub>2.5</sub>	PM <sub>2.5–10</sub>	PM <sub>10</sub>
<i>North Taiwan</i>					
Urban	SP	$3.8 \times 10^{-3} \pm 4 \times 10^{-4}$	$0.48 \pm 0.16$	$0.22 \pm 0.01$	$0.24 \pm 0.02$
	CRSP	$8.2 \times 10^{-3} \pm 8 \times 10^{-4}$	$0.60 \pm 0.11$	$0.28 \pm 0.03$	$0.31 \pm 0.04$
Suburban	SP	$3.8 \times 10^{-3} \pm 4 \times 10^{-4}$	$0.50 \pm 0.01$	$0.32 \pm 0.08$	$0.49 \pm 0.02$
	CRSP	$8.2 \times 10^{-3} \pm 8 \times 10^{-4}$	$0.65 \pm 0.01$	$0.49 \pm 0.10$	$0.64 \pm 0.02$
<i>Central Taiwan</i>					
SO <sub>4</sub> <sup>2-</sup>	SP	$2.9 \times 10^{-3} \pm 3 \times 10^{-4}$	$0.39 \pm 0.03$	$0.22 \pm 0.03$	$0.37 \pm 0.03$
	CRSP	$6.4 \times 10^{-3} \pm 7 \times 10^{-4}$	$0.43 \pm 0.02$	$0.35 \pm 0.14$	$0.42 \pm 0.03$
NO <sub>3</sub> <sup>-</sup>	SP	$2.9 \times 10^{-3} \pm 3 \times 10^{-4}$	$0.28 \pm 0.06$	$0.27 \pm 0.10$	$0.27 \pm 0.08$
	CRSP	$6.4 \times 10^{-3} \pm 7 \times 10^{-4}$	$0.35 \pm 0.02$	$0.36 \pm 0.04$	$0.35 \pm 0.03$

<sup>a</sup>Surface area-to-volume ratio ( $A/V$ ) = 1.00 m<sup>-1</sup>.

<sup>b</sup>Mean deposition rate ( $\lambda_d(k)$ ) for PM<sub>2.5</sub>, PM<sub>2.5–10</sub> and PM<sub>10</sub> are  $8.6 \times 10^{-3}$ , 0.43, and 0.67 h<sup>-1</sup>, respectively.

the CRSP-type building. Generally, PM<sub>2.5</sub> mass has higher mass I/O ratios than that of PM<sub>2.5–10</sub> and PM<sub>10</sub> for both SP- and CRSP-type buildings (Table 5), suggesting much more effective penetration of fine than coarse PMs from outdoors into house. Little studies containing suitable data were identified; thus extremely limited empirical evidence was available for model validation, especially for the wind-induced naturally ventilated residences in Taiwan region. Monn et al. [28] reported that the average mass I/O ratios for PM<sub>2.5</sub> and PM<sub>10</sub> were 0.54 and 0.69, respectively, for the naturally ventilated homes without any indoor sources and where human activity was low. Our average PM<sub>2.5</sub> mass I/O ratio prediction of  $0.56 \pm 0.07$  matched well with measured PM<sub>2.5</sub> I/O ratio of 0.54, yet had lower PM<sub>10</sub> I/O ratio ( $0.42 \pm 0.16$ ) than that of Monn et al. [28] of 0.69.

Our results also show that coarse PMs have larger deposition velocities (deposition rate divided by the surface area-to-volume ratio equals the deposition velocity) than fine PMs, which leads to a reduction in their indoor concentrations as they fall out by gravitational settling or deposit on window and door frames (i.e., larger deposition velocities induce higher deposition fluxes). In our work, the average deposition rates for PM<sub>2.5</sub> and PM<sub>10</sub> are 0.009 and 0.67 h<sup>-1</sup>, respectively. These deposition rates are equivalent to deposition velocities of 0.009 and 0.67 m h<sup>-1</sup> corresponding to a surface area-to-volume of 1.00 m<sup>-1</sup> in the present study. Wallace [29] reviewed the indoor air quality literature and reported that average I/O mass concentration ratios for PM<sub>2.5</sub> and PM<sub>10</sub> were 0.67 and 0.57, respectively, and average deposition rates of 0.39 and 0.65 h<sup>-1</sup> for PM<sub>2.5</sub> and PM<sub>10</sub>, respectively. Assuming a surface area-to-volume ratio of 1.00 m<sup>-1</sup>, these deposition rates are equivalent to deposition velocities of 0.39 and 0.65 m h<sup>-1</sup>, respectively. Their fitted PM<sub>10</sub> deposition rate is consistent with that found in the present study. Their integrated PM<sub>2.5</sub> deposition rate,

however, is about 40 times larger than our predictions. The discrepancy may be due to differences in the outdoor particle size distribution or the inclusion of indoor sources in the data employed by Riley et al. [23].

These differences suggest that care must be taken when choosing representative values for exposure assessment. We suggest that a mathematical relationship between air-exchange rate and deposition velocity can be developed to eliminate the limitations. Furtaw et al. [30] demonstrated that the amount of turbulence in a room is proportional to the air-exchange rate. Accordingly, an increase in turbulence will increase the particle deposition rate [19,31]. These factors will lead to the increase in deposition velocity for all particle sizes as air-exchange rate increases.

In a single residence study, Thatcher and Layton [22] calculated the deposition velocities between 0.64 and 4.15 m h<sup>-1</sup> for 1–6 μm AED particles. In several residences, Fogh et al. [32] measured particle deposition velocities between 0.18 and 1.1 m h<sup>-1</sup> for particle AED between 0.5 and 5.5 μm in that calculated I/O mass concentration ratios varied between 0.1 and 0.7 for the same sized particles. In an enclosed chamber, Lewis [33] experimentally measured the deposition rates between 0.25 and 1.1 h<sup>-1</sup> for particle AED between 1 and 7 μm. Lewis [33] also demonstrated that increasing the pressure differential or aperture of an opening increased the penetration for all particle sizes. Riley et al. [23] used deposition rates ranged from 0.09 to 0.33 h<sup>-1</sup> and 0.17 to 2.1 h<sup>-1</sup> for PM<sub>2.5</sub> and PM<sub>10</sub>, respectively, to estimate the PM mass I/O ratios.

Fig. 5 gives the outdoors and predicted indoors number, surface area, and volume concentration distributions of sulfate and nitrate in the central Taiwan region for the SP- and CRSP-type buildings. Since they have similar particle size distributions (Fig. 2), the sulfate and nitrate

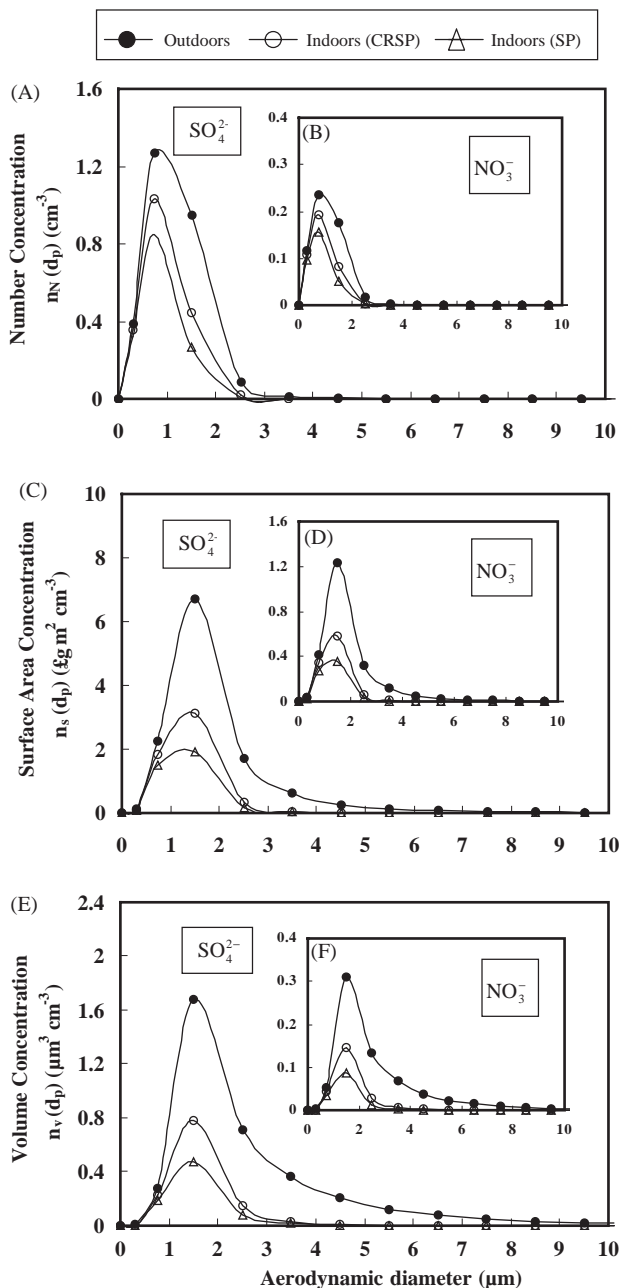


Fig. 5. Outdoor PM distributions and predicted indoor PM number, surface area, and volume concentrations of chemical fractions of sulfate and nitrate for the Sp- and CRSP-type buildings in central Taiwan region. (A, C, E) show the number, surface volume, and volume distributions, respectively, for sulfate PM; (B, D, F) show the corresponding distributions for nitrate PM.

distributions have the similar patterns of behavior (Fig. 5). A relatively large portion of the sulfate volume concentration is removed by the order of magnitude of  $10^1$  as compared to the nitrate volume concentration (Figs. 5e, f). The SP-type building reduces the indoor surface area and volume concentrations of sulfate and nitrate more efficiently than that of the CRSP-type building. Much of the indoor surface area and volume distributions of sulfate and nitrate

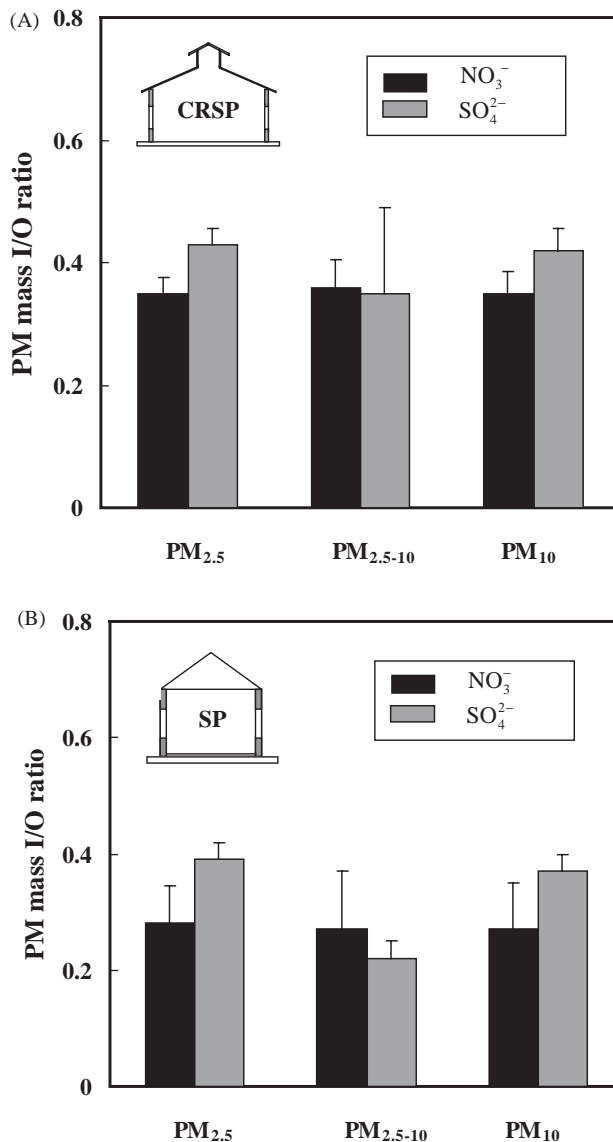


Fig. 6. Predicted PM mass I/O ratios of sulfate and nitrate PM<sub>2.5</sub>, PM<sub>2.5–10</sub>, and PM<sub>10</sub> for (A) the SP- and (B) the CRSP-type buildings in central Taiwan region. The error bars show the standard deviation from the mean.

is below particle AED of 3 μm, in which air-exchange rate is an efficient removal mechanism (Figs. 5c–f).

Fig. 6 illustrates the PM mass I/O ratios predictions for PM<sub>2.5</sub>, PM<sub>2.5–10</sub>, and PM<sub>10</sub> fractions of sulfate and nitrate in central Taiwan region for Sp- and CRSP-type buildings. Building differences have an impact on the PM mass I/O ratios for both constituents. Generally, the SP-type building has lower PM mass I/O ratios than that of the CRSP-type building. Values range from 0.22 sulfate PM<sub>2.5–10</sub> I/O ratio for the SP-type building to 0.43 sulfate PM<sub>2.5</sub> I/O ratio for the CRSP-type building (Table 5). In general, both the SP- and CRSP-type buildings lowered the PM mass I/O ratios for both species below 0.5 (Table 5).



#### 4. Conclusions

This paper illustrates the use of a simple yet robust size-dependent indoor air quality model on PM I/O relationships and PM loss mechanisms within a wind-induced naturally ventilated building. We determined the natural ventilation by an opening effectiveness model for a wind-induced naturally ventilated airspace, in which the commonly employed sidewall openings and covered ridge with sidewall openings were our scale models. Using a well-established mass balance model incorporation with the outdoor PM measurements and literature information on outdoors PM chemical profiles, we have shown that PM mass indoor/outdoor (I/O) ratios can vary from 0.22 to 0.65, whereas for the sulfate and nitrate PM mass I/O ratios ranged from 0.22 to 0.43.

The most significant removal mechanisms included natural ventilation through and particle deposition on indoor surfaces. The modeled PM I/O concentration ratios depend on ambient size distributions of the PM metric and building designs that influence the opening effectiveness and thus have a significant effect on the estimates of human exposure. The present work can prompt the research on the relationships between PM concentrations and exposures, and subsequently adverse health responses assessment. Since individuals may spend more than 80% of their time indoors, understanding the relationship between outdoor PM concentrations and those found in indoor microenvironments is critical.

Our results suggest that we may modify indoor PM exposures through a risk-reduction strategy by changing building design and operation of ventilation systems. To improve the model, additional experimental evidence is needed to characterize the distributional profiles of indoor generation sources and deposition velocities as a function of particle size in relation to air-exchange rates of the natural ventilation system.

#### References

- [1] Pope CA, Dockery DW. Acute health effects of PM<sub>10</sub> pollution on symptomatic and asymptomatic children. *American Review of Respiratory Disease* 1992;145:1123–8.
- [2] Dockery DW, Pope CA, Xu XP, Spengler JD, Ware JH, Fay ME, Ferris BG, Speizer FE. An association between air pollution and mortality in 6 united states. *New England Journal of Medicine* 1993;329:1753–9.
- [3] Schwarz J. Particulate air pollution and chronic respiratory disease. *Environment Research* 1993;62:7–13.
- [4] Seaton A, MacNee W, Donaldson K, Godden D. Particulate air pollution and acute health effects. *Lancet* 1995;345:176–8.
- [5] Ackermann-Lieblich UA, Leuenberger Ph, Scwartz J, Schindler C, Monn C, Sapaldia T. Lung function and long term exposure to air pollutions in Switzerland. *American Journal of Respiratory and Critical Care Medicine* 1997;155:122–9.
- [6] Guo Y, Lin YC, Sung FC, Huang SL, Ko YC, Lai JS, Su HJ, Shaw CK, Lin RS, Dockery DW. Climate, traffic-related air pollutants, and asthma prevalence in middle-school children in Taiwan. *Environmental Health Perspectives* 1999;107:1001–6.
- [7] Hwang JS, Chan CC. Effects of air pollution on daily clinic visits for lower respiratory tract illness. *American Journal of Epidemiology* 2002;155:1–10.
- [8] Chen WC, Wang CS, Wei CC. An assessment of source concentrations to ambient aerosol in Central Taiwan. *Journal of the Air and Waste Management Association* 1997;47:501–9.
- [9] Yang HH, Chiang CF, Hee WJ, Hwang KP, Wu EM. Size distribution and dry deposition of road dust PAHs. *Environment International* 1999;25:585–97.
- [10] Fang GC, Chang CN, Wu YS, Fu PPC, Yang DG, Chu CC. Characterization of chemical species in PM<sub>2.5</sub> and PM<sub>10</sub> aerosol in suburban and rural sites of central Taiwan. *The Science of the Total Environment* 1999;234:203–12.
- [11] Chen ML, Mao IF, Lin IK. The PM<sub>2.5</sub> and PM<sub>10</sub> particles in urban area of Taiwan. *The Science of the Total Environment* 1999;226:227–35.
- [12] Chiou SF, Tsai CJ. Measurement of emission factor of road dust in a wind tunnel. *Powder Technology* 2001;118:10–5.
- [13] Lu HC. The statistical characters of PM<sub>10</sub> concentration in Taiwan area. *Atmospheric Environment* 2002;36:491–502.
- [14] Li CS, Lin CH. PM<sub>1</sub>/PM<sub>2.5</sub>/PM<sub>10</sub> characteristics in the urban atmosphere of Taipei. *Aerosol Science and Technology* 2002;36:469–73.
- [15] de Jong T, Bot GPA. Air exchange caused by wind effects through (window) openings distributed evenly on a quasi-infinite surface. *Energy and Buildings* 1992;19:93–103.
- [16] Miguel AF, van de Braak NJ, Silva AM, Bot GPA. Wind-induced airflow through permeable materials part I: air infiltration in enclosure. *Journal of Wind Engineering and Industrial Aerodynamic* 2001;89:59–72.
- [17] ASHRAE handbook of fundamentals. Atlanta, GA: American Society of Heating, Refrigerating and Air Conditioning Engineers; 1997.
- [18] Miguel AF. Airflow through porous screen: from theory to practical considerations. *Energy and Buildings* 1998;28:63–9.
- [19] Crump JG, Seinfeld JH. Turbulent deposition and gravitational sedimentation of an aerosol in a vessel of arbitrary shape. *Journal of Aerosol Science* 1981;12:405–15.
- [20] Abt E, Suh HH, Catalano P, Koutrakis P. Relative contribution of outdoor and indoor particle sources to indoor concentrations. *Environmental Science and Technology* 2000;34:3579–87.
- [21] Jones NC, Thornton C, Mark D, Harrison RM. Indoor/outdoor relationships of particulate matter in domestic homes with roadside, urban and rural locations. *Atmospheric Environment* 2000;34:2603–12.
- [22] Thatcher TL, Layton DW. Deposition, resuspension, and penetration of particles within a residence. *Atmospheric Environment* 1995;29:1487–97.
- [23] Riley WJ, McKone TE, Lai AK, Nazaroff WW. Indoor particulate matter of outdoor origin: importance of size-dependent removal mechanisms. *Environmental Science and Technology* 2002;36:200–7.
- [24] Liao CM, Chen JW, Huang MY, Chen JS, Chang TJ. An inhalation dose model for assessing dust-borne VOC-odor exposure from feeding in swine buildings. *Transactions of the ASAE* 2001;44:1813–24.
- [25] Lai AK, Nazaroff WW. Modeling indoor particle deposition from turbulent flow onto smooth surfaces. *Journal of Aerosol Science* 2000;31:463–76.
- [26] Yu H, Hou CH, Liao CM. Scale model analysis of opening effectiveness for wind-induced natural ventilation openings. *Biosystems Engineering* 2002;82:199–207.
- [27] Chang KF, Fang GC, Lu CS, Bai HL. Particle size distribution and anion content at a traffic site in Sha-Lu, Taiwan. *Chemosphere* 2001;45:791–9.

- [28] Monn C, Fuchs A, Hogger D, Junker M, Kogelschatz D, Roth N, Wanner HU. Particulate matter less than 10  $\mu\text{m}$  (PM10) and fine particles less than 2.5  $\mu\text{m}$  (PM2.5): relationships between indoor, outdoor and personal concentrations. *The Science of the Total Environment* 1997;228:15–21.
- [29] Wallace L. Indoor particles: a review. *Journal of the Air and Waste Management Association* 1996;46:98–126.
- [30] Furtaw EJ, Pandian MD, Nelson DR, Behar JV. Modeling indoor air concentrations near emission sources in imperfectly mixed rooms. *Journal of the Air and Waste Management Association* 1996;46: 861–8.
- [31] Nazaroff WW, Cass GR. Mass-transport aspects of pollution removal at indoor surface. *Environment International* 1989;15:567–84.
- [32] Fogh CL, Byrne MA, Roed J, Goddard AH. Size specific indoor aerosol deposition measurements and derived I/O concentrations ratios. *Atmospheric Environment* 1997;31:2193–203.
- [33] Lewis S. Solid particle penetration into enclosure. *Journal of Hazardous Materials* 1995;43:195–216.
- [34] Hinds WC. *Aerosol technology: properties, behavior, and measurement of airborne particles*, 2nd ed. New York, NY: Wiley; 1999.